Desalination and Water Treatment
www.deswater.com

doi: 10.5004/dwt.2017.20728

75 (2017) 132–147
May

Removal of Cu(II) and Cd(II) ions from aqueous solutions using local raw material as adsorbent: a study in binary systems

Necla Caliskan[a,*], Eda Gokirmak Sogut[b], Ali Savran[a], Ali Riza Kul[a], Senol Kubilay[a]

[a]*Department of Physical Chemistry, Faculty of Science, Yüzüncü Yıl University, 65080 Van, Turkey, Tel. +90 4322251806/22283; Fax: +90-4322251802; emails: ncaliskan7@hotmail.com (N. Caliskan), alisavran38@hotmail.com (A. Savran), alirizakul@yyu.edu.tr (A.R. Kul), senolkubilay@yyu.edu.tr (S. Kubilay)*
[b]*Van Security School, Yüzüncü Yıl University, 65080 Van, Turkey, email: edagokirmak@hotmail.com*

Received 11 October 2016; Accepted 21 March 2017

ABSTRACT

The purpose of this study is to examine the interaction of Cu(II) and Cd(II) ions in solution with the local raw clayey material of Tilkitepe located in the eastern shore of Lake Van in East Anatolia (Turkey). This material was used as an adsorbent without any chemical or physical treatment and was characterized by X-ray fluorescence, X-ray diffraction, scanning electron microscope, Fourier transform infrared and differential thermal analysis–thermogravimetric analyses. Langmuir, Freundlich, Dubinin–Kaganer–Radushkevich, Temkin and Harkins–Jura non-linear adsorption isotherm models were applied to the experimentally obtained adsorption data and the isotherm constants were calculated. The highest R^2 values for adsorption of both ions in the binary system were obtained by applying the experimental data to the Freundlich isotherm model. In binary system, the experimental adsorption capacities for Cu(II) and Cd(II) ions obtained by kinetic data were 52.631 and 44.843 mg g^{-1} at 600 mg L^{-1} initial metal ion concentrations, respectively. In the competitive adsorption, the affinity of Cu(II) toward the adsorbent was much higher than that of the Cd(II). Adsorption kinetics was evaluated using the pseudo-first-order, pseudo-second-order, intraparticle diffusion, Avrami and mass transfer kinetic models. The experimental data proved a closer fit to the pseudo-second-order model. Thermodynamic parameters such as enthalpy ($\Delta H°$), Gibbs free energy ($\Delta G°$) and entropy ($\Delta S°$) were calculated using adsorption isotherms obtained at different temperatures. The results show that the adsorption is spontaneous and controlled by a physical mechanism.

Keywords: Competitive adsorption; Heavy metal; Raw clay; Non-linear isotherm models; Thermodynamic; Kinetic

1. Introduction

Metals are naturally present in our environment and trace amount of metals is essential micronutrients for growth of many organisms. But, their excess quantity can be toxic to life in the environment [1]. Increasing concerns about the protection of the natural environment in industrialized societies has accelerated research on the formation and elimination of heavy metals in soils, water sources and wastes [2]. These substances which are extremely harmful to human health are a result of the intended use of heavy metals in industrial products. Many technological methods used to prevent heavy metal contamination such as ion exchange and adsorption [3]. Adsorption has been recognized as one of the most generally used system for the decontamination owing to its ease, stable treatment process, the lack of secondary pollution and lower price [4]. Principally, any solid having a porous structure can be selected as an adsorbent, e.g., clays and clay minerals, inorganic oxides (ferric oxide, titanium oxide, etc.), zeolites, alumina, silica gel, activated carbon, soil, river sediment [5,6] and natural materials like wood, peat, coal and lignite. In selecting adsorbent, other parameters like production cost, accessibility, environmental adaptability, energy

* Corresponding author.

expenses should be determined apart from the adsorption capacity of material [7]. The clays are hydrated aluminum or magnesium silicates as usually described that constitute colloidal segment (<2 μm) of soils and may consist of combinations of fine grained clay minerals and non-clay minerals, e.g., quartz, calcite and metal oxides [8]. Naturally occurring clays have good potential in the elimination of heavy metals from aqueous solution because of their physicochemical properties, extensively availability, not poisonous or toxic, chemical and mechanical stability, Brønsted and Lewis acidity compared with several conventional adsorbents [9,10]. Adsorption of heavy metal ions is concerned with charge features of the clay. Charge characteristics of adsorbent contain the size of the active sites and cation exchange capacity which has two factors; i.e., permanent negatively charged site caused by isomorphous substitution in the octahedral and tetrahedral sheets of the silicate layers and variable-charge sites resulting from dissociation of edge hydroxyl groups [11]. Clays are often used as a natural barrier against the harmful effects of toxic waste [12]. The use of natural clay without any pretreatment as industrial material is economically more sustainable method. In addition, secondary pollution caused by pretreatment is prevented. In most cases, the nature of clay that seals the site floor is a criterion for selecting the landfill site [13]. Determination of the adsorption properties of natural clay has a fundamental importance to evaluate the potential use as a storage barrier material [14]. In recent years, the search for locally available clays as low-cost adsorbents has been intensified [15]. Van lake basin is rich in some industrial raw materials. The clayey soils in the region are important raw material reserves used in the production of ceramics in ancient times and used today by the people of the region for personal cleaning applications. Apart from a study investigating their use as bricks and tiles, Ateş and Yakupoğlu [12] reported that, clays in the basin have suitable properties to be used as liner materials. Although the Lake Van Basin has significant clayey soil formation, the removal of heavy metal pollution by these natural basin clayey materials has not been explored. For this reason, this study aims to present the obtained data about whether the raw clayey material can be used as an adsorbent. It is very important that the raw material is to be used without any pretreatment that is to say without secondary energy expenditure and chemical waste.

The Lake Van Basin including the lake at its center has an area of 19,500 km^2, with its longest dimensions extending to 200 km in the east–west and 170 km in the north–south direction [12]. More than half of the population in the basin lives along the edge of the stream and on the coast of the lake. In recent years, the populations of the towns in the basin have risen rapidly because of migrations from rural to urban centers; however, enough urban infrastructures have not been able to be made up parallel to this rapid population growth. Urban wastes have generally been discharged into the lakes and streams without being refined. This situation causes a serious environmental pollution in the basin. In addition, the use of low quality coal as fuel in the region causes intense air pollution.

This study focuses on two heavy metal, cadmium [16] and copper [17]. These are elements of the first and second classes of ecological hazard [18]. According to the US Environmental Protection Agency (EPA), the major sources of cadmium in the air are the burning of fossil fuels such as coal, oil or the disposal of municipal waste. The harmful effect of cadmium on human health mainly occurs as lung irritation and its compounds are compared with other heavy metals, fairly water soluble. Therefore, cadmium ions accumulate and can easily contaminate soil. Copper is microelement essential for living organisms. However, the US EPA has determined that copper is harmful to human health because of the health effects such as liver or kidney damage when people are exposed to it at levels above the action level (1.3 ppm).

Most of the studies on removal of heavy metals using adsorbents are performed for a single metal solution. However, the presence of a toxic metal ion in natural water and wastewater is a rare condition. In natural environment, a large number of metal ions usually occur together and compete for the available adsorption sites of adsorbent. Also, the presence of other metal ions can lead to synergism, antagonism or non-interaction [19].

In this study, the raw material sample was collected as a natural resource in the vicinity of the archaeological site Tilkitepe at the eastern shore of Lake Van in East Anatolia (Turkey) and has been characterized. The prehistoric settlement of Tilkitepe (sixth to third millennium BC) is located within the Van Airport boundaries, about 6 km south of Tushpa, the capital city of Urartian Kingdom (ninth to sixth century BC) [20]. The raw clay was tested to explore their adsorptive potential for the removal of cadmium and copper ions in the binary system. It is necessary to have information about the effect of system parameters under varying process conditions to identify the physicochemical conditions which are most effective for the removal of metal ions from wastewater. This is required for optimum system design criteria because wastewaters from different metallurgical and chemical processes may contain mixtures of metals and other waste compounds [21]. Optimum sorption conditions were determined as a role of initial metal ions concentration, contact time, temperature and pH. The equilibrium adsorption isotherm studies are basically vital in design of treatment systems. The competitive adsorption equilibrium isotherms of Cu(II) and Cd(II) ions in aqueous solution on raw material have been studied by the batch technique. Non-linear isotherm method has been used to predict the optimum adsorption isotherm and also to obtain the isotherm parameters. This method is based on minimizing the error distribution between the experimental data and the predicted isotherm. To evaluate isotherm data, many error functions such as non-linear chi-square (χ^2) test, standard error (SE) and R^2 are used [22]. Also, thermodynamic parameters determined and pseudo-first-order, pseudo-second-order, intraparticle diffusion, Avrami and mass transfer kinetic models were applied in order to describe the adsorption mechanism and the characteristic constants of the adsorption process.

2. Materials and methods

2.1. Materials

The raw material sample collected from region was powdered in a porcelain mortar to obtain finer grains. The sample was milled passing 230 mesh sieve (62.0 μm) to eliminate the formation of lump. Before the experiments

the powdered raw material was dried at room temperature for at least 2 weeks. The pore diameter is found to be 21.756 and 17.686 Å, respectively, by Barrett–Joyner–Halenda (BJH) adsorption and desorption method. This method is used to determine the pore size distribution of a mesoporous solid material based on the conventional Kelvin equation. BJH analysis can also be used to determine pore area, mean pore diameter and specific pore volume by using adsorption and desorption techniques [23].

The sample was directly used in the analysis without being subjected to any process mineral enrichment. Quantitative chemical analysis of material obtained by X-ray fluorescence spectrometer (XRF; Philips 2400) technique shown that the raw sample contains mainly of SiO_2 37.5%, and it has 20.5% CaO, 6.2% MgO, 5.6% Al_2O_3, 5.4% Fe_2O_3, 0.6% TiO_2, 2.0% Na_2O, 1.3% K_2O, 0.1% MnO and 0.1% P_2O_5. In addition, the trace elements in raw material are given in Table 1.

2.2. Sample characterization

Mineralogical composition of the sample was characterized by X-ray diffraction (XRD; Philips PW 1830-40) with a Cu Kα radiation. Morphology of sample was obtained by scanning electron microscope (SEM; LEO 440 computer controlled digital). Molecular structure was investigated by Fourier transform infrared (FTIR) spectrometer (Bio-Rad Win-IR). Brunauer–Emmett–Teller (BET) surface area measurement was performed on a Nova 2200e Quantachrome Instruments surface area analyzer. Specific surface area of raw clay is determined as 45 $m^2 g^{-1}$ using the method.

Table 1
Trace elements (ppm)

F	<1,500
Sc	<20
V	89
Cr	440
Co	<50
Ni	238
Cu	<30
Zn	58
Rb	38
Sr	669
Y	20
Zr	804
Nb	<20
Ba	114
La	<40
Pb	<20
Nd	<20
Yb	<15
Th	<15
U	<15

Thermal analysis (thermogravimetric–differential thermal analysis [TG–DTA]) was made by Rigaku 2.22E1 Thermal Analyzer Instrument under given operating criteria: heating from 10°C to 1,099°C at a rate of 20°C min^{-1} in atmospheric air.

2.3. Batch experiments

The interaction between adsorbent and heavy metal ions were investigated using batch technique. Stock solutions with the same concentration of Cd(II) and Cu(II) were prepared using $Cd(NO_3)_2$ and $Cu(NO_3)_2$ as the sources of heavy metal ions, respectively. The experiments were performed by mixing 0.1 g of clay sample with 10 mL metal-nitrate solutions including different initial concentrations of the metal ions solution (50, 75, 100, 150, 200, 250, 300, 400, 500 and 600 mg L^{-1}). The initial concentrations of Cu(II)–Cd(II) ions in binary metal solution were arranged to be equal. All chemicals used were of analytical grade and solutions were prepared using doubly distilled water. The obtained mixtures were shaken in a thermally controlled automatic shaker at 110 rpm at temperatures of 298, 308 and 318 K for different contact time periods (1–150 min intervals) until equilibrium conditions had been reached. In any case, a contact time of 110 min was found to be sufficient to reach adsorption equilibrium. The amount of metal ions adsorbed onto the clay was calculated by the difference between the initial and the final metal concentrations obtained using Solaar AA M series v1, 23 model (Thermo Scientific, UK) atomic absorption spectrometry. The experiments were repeated at least twice under the same conditions and the reproducibility was observed. The amount of adsorbed metal ions was calculated from the following equations [24]:

$$q_e = \frac{(C_i - C_e)V}{m} \quad (1)$$

where q_e is the amount of metal ions adsorbed (mg g^{-1}) at the equilibrium time, V is the volume of the solution (L), m is the weight of the adsorbent (g), and C_i and C_e are the metal ion concentrations (mg L^{-1}) at the initial and equilibrium times, respectively. The batch adsorption tests were carried out at pH 5.5. These measurements were made using a WTW pH meter (Series 720, Germany).

2.4. Adsorption isotherms

It is defined that the adsorption isotherm is the relationship between the equilibrium pressure or concentration and the amount adsorbed by the adsorbent material at a constant temperature [25]. In this study, the experimental equilibrium data of the investigated metal ions on adsorbent were analyzed by the five non-linear isotherm models, i.e., the Langmuir [26], Freundlich [27], Dubinin–Kaganer–Radushkevich (DKR) [28], Temkin [29] and Harkins–Jura [30] isotherms. Linear forms of the isotherms models are usually accepted to determine the isotherm parameters or the most appropriate model for the adsorption system due to the mathematical convenience [31]. However, more accurate results can be obtained by the non-linear regression method because the error distribution cannot be changed as in linear technique [32]. Experimentally

determined q_e and C_e values are applied to non-linear equations of adsorption isotherms. Using the Origin 8.0 software, the experimental results (points) and the theoretically calculated values from the equations are plotted on the same axes. All parameters of the isotherm models are assessed by non-linear regression method using this software [31]. The correlation coefficient (R^2), SE for each parameter (the standard deviation of a distribution of a sample statistic) and χ^2 values were used to select the best theoretical isotherm. The correlation coefficient is a value that is used to show the relationship between variables. The percentage degree varies from 0 to 1 [33]. Non-linear χ^2 test is an arithmetical implement necessary for the best fit of a sorption system. Small χ^2 values show its similarities while larger values emphasize the deviation of the experimental data [34]. These parameters are determined in the following Eqs. (2) and (3) [35]:

$$R^2 = \frac{\sum(q_{e,\text{calc}} - \overline{q_{e,\text{exp}}})^2}{\sum(q_{e,\text{calc}} - \overline{q_{e,\text{exp}}})^2 + \sum(q_{e,\text{calc}} - q_{e,\text{exp}})^2} \quad (2)$$

$$\chi^2 = \sum_{i=1}^{N} \frac{(q_{e,\text{exp}} - q_{e,\text{calc}})^2}{q_{e,\text{calc}}} \quad (3)$$

where $q_{e,\text{exp}}$ (mmol g^{-1}) is determined from the batch experiment, $q_{e,\text{calc}}$ (mmol g^{-1}) calculated value from the isotherm for corresponding $q_{e,\text{exp}}$, $\overline{q_{e,\text{exp}}}$ is the average of $q_{e,\text{exp}}$ and N is the number of observations in the experimental data. The small SE values indicate that the adsorption isotherms best fit [36].

The non-linear equations and parameters of these models are presented in Table 2.

Langmuir isotherm is based on the mono-molecule thickness of the adsorption because intermolecular interaction forces are weak when moving away from the solid surface (solid, liquid or gas) [37]. The dimensionless separation factor (R_L) is calculated by using Langmuir constant (k_L) and given by the following Eq. (4):

$$R_L = \frac{1}{1 + k_L C_i} \quad (4)$$

where C_i is the initial metal concentration (mmol L^{-1}). The value of R_L shows the type of the isotherm to be either unfavorable ($R_L > 1$), linear ($R_L = 1$), favorable ($0 < R_L < 1$) or irreversible ($R_L = 0$) [19]. The Freundlich isotherm is designed as an empirical isotherm showing the surface heterogeneity of the adsorbent. K_F and n (dimensionless) are the Freundlich adsorption isotherm constants depending on the temperature, adsorbent and the adsorbed compound. The constants express the magnitude of adsorption capacity and the degree of adsorption indicating the adsorption intensity, respectively [3]. If $n = 1$, then the partition between the two phases are independent of the concentration. If $1/n$ value is less than one it shows a normal adsorption. Conversely, if $1/n$ is greater than one indicates that the cooperative adsorption [38].

Dubinin–Kaganer–Radushkevich isotherm is often used to describe the adsorption mechanism with a Gaussian energy distribution onto a heterogeneous surface [38]. The constant β provides an idea about the mean free energy

Table 2
Non-linear isotherm models

Isotherm	Equation	Constants	Reference
Langmuir	$q_e = \frac{q_m K_L C_e}{1 + K_L C_e}$	K_L is the Langmuir isotherm constant (L g^{-1}) C_e is the equilibrium concentration of adsorbate (mg L^{-1}) q_e is the amount of metal adsorbed per gram of the adsorbent at equilibrium (mg g^{-1})	[24]
Freundlich	$q_e = K_F C_e^{\frac{1}{n}}$	K_F is the Freundlich isotherm constant (L g^{-1}) n is the heterogeneity factor in the Freundlich model	[25]
Dubinin–Kaganer–Radushkevich	$q_e = q_m \exp(-\beta\varepsilon^2)$ $\varepsilon = RT\ln\left(1 + \frac{1}{C_e}\right)$ $E = 1/(2\beta)^{1/2}$	β is a constant associated to the mean free energy of adsorption per mole of the adsorbate (mol^2 J^{-2}) q_m is the theoretical saturation capacity ε is the Polanyi potential E is energy of adsorption (kJ mol^{-1}) R is the ideal gas constant (8.314 J mol^{-1} K^{-1})	[26]
Temkin	$\frac{q_e}{q_m} = \theta = \frac{RT}{b_T}\ln(A_T C_e)$	A_T is the Temkin isotherm equilibrium binding constant (L g^{-1}) b_T is the Temkin isotherm constant B_T is the constant related to heat of sorption (J mol^{-1}) R is the ideal gas constant (8.314 J mol^{-1} K^{-1}) T is the temperature (K)	[27]
Harkins–Jura	$q_e = \left(\frac{A}{B - \log C_e}\right)^{1/2}$	B is the isotherm constant A is the Harkins–Jura isotherm parameter	[28]

E (kJ mol^{-1}) of adsorption and can be computed using the equation in Table 2 [39]. If the energy (E) <8 kJ mol^{-1}, adsorption can be explained with physical interactions. Conversely, if the energy >8 kJ mol^{-1}, adsorption mechanism can be defined with chemical interactions [39].

The Temkin isotherm model is ideal to predict the gas phase equilibrium; on the other hand complex adsorption systems containing the liquid-phase adsorption isotherms are generally not suitable to be exemplified [34]. Temkin adsorption isotherm non-linear equation is presented in Table 2 [29]. B_T is a constant associated with heat of sorption (J mol^{-1}) and it is determined using Eq. (5) [38].

$$B_T = \frac{RT}{b_T} \tag{5}$$

The applicability of the Langmuir and BET isotherms is limited. The Harkins–Jura adsorption isotherm is advanced for solution-solid systems on the assumption that the adsorbed film is of the condensed form [40]. In addition, this isotherm equation refers to multilayer adsorption and can be clarified by the presence of a heterogeneous pore distribution. A is Harkins–Jura isotherm parameters of multilayer adsorption and B is the isotherm constant [41].

2.5. Adsorption kinetics

Adsorption phenomenon is a time-dependent process. To accomplish the design of the adsorption system, the mechanism and kinetics of adsorption must be known. Kinetic models are used to determine the adsorption mechanism and adsorption time. Batch experiments were analyzed using pseudo-first-order (Eq. (6)), pseudo-second-order (Eq. (7)), intraparticle diffusion (Eq. (8)), Avrami (Eq. (9)) and mass transfer (Eq. (10)) model kinetics [42,43]:

$$\log(q_e - q_t) = \log q_e - \frac{kt}{2.303} \tag{6}$$

$$\frac{t}{q_t} = \frac{1}{k_2 q_e^2} + \frac{t}{q_e} \tag{7}$$

where q_e and q_t are the amount of solute adsorbed per unit amount of adsorbent at equilibrium and any time, t, respectively (mg g^{-1}), k_1 is the pseudo-first-order rate constant (min^{-1}) and k_2 is the pseudo-second-order rate constant (g mg^{-1} min^{-1}).

$$q_t = k_i t^{1/2} + C \tag{8}$$

where k_i is the intraparticle diffusion rate constant (mg g^{-1} min$^{-0.5}$) and is linearized Avrami equation:

$$\ln\left[-\ln\frac{1-q_t}{q_e}\right] = n\ln k + n\ln t \tag{9}$$

where k is the Avrami kinetic constant (min^{-1}) and n may be associated with the reaction mechanism for a wide range of solid-state reactions. Values of $n < 1$ are related to diffusion mechanisms, whereas values >1 show that the rate of reaction is controlled by the speed of the phase boundary [44].

For calculation of the mass transfer coefficient, it is assumed that in a well agitated adsorber, the mixing in the liquid phase is rapid and so the concentration of heavy metal ions in the liquid phase and the concentration m of adsorbent particles in the liquid are nearly uniform throughout the vessel [45].

Mass transfer coefficient, β (m s^{-1}) of Cu(II) and Cd(II) ions at the adsorbent–solution interface were determined by using Eq. (10) [46]:

$$\ln\left(\frac{C_t}{C_i} - \frac{1}{1+mK}\right) = \ln\left(\frac{mK}{1+mK}\right) - \left(\frac{1+mK}{mK}\right)\beta S t \tag{10}$$

where m is the mass of adsorbent (g), K is the Langmuir constant (L g^{-1}), S is the surface area of adsorbent (m^2 g^{-1}) and time (t).

2.6. Thermodynamic parameters

In the temperature-dependent adsorption studies, thermodynamics parameters of adsorption provide valuable information to understand the process completely. The values of free energy (ΔG°), enthalpy (ΔH°) and entropy (ΔS°) were calculated using the following equations.

The apparent equilibrium constant (K'_c) of the sorption is defined as:

$$K'_c = \frac{C_{\text{ad,eq}}}{C_{\text{eq}}} \tag{11}$$

$$\ln K_c° = -\frac{\Delta H°}{RT} + \frac{\Delta S°}{R} \tag{12}$$

$$\Delta G° = \Delta H° - T\Delta S° \tag{13}$$

where $C_{\text{ad,eq}}$ is the concentration of metal ion on the adsorbent at equilibrium. This situation can be used instead of concentration with the aim of obtaining the standard thermodynamic equilibrium constant (K_c°) of the sorption system [47]. R is the universal gas constant (8.314 J mol^{-1} K^{-1}) and T is temperature (K). ΔH° and ΔS° values can be obtained from the slope and intercept of Van't Hoff plots of lnK_c° vs. 1/T [48,49]. ΔG° values are calculated using Eq. (13) for each temperature.

3. Results and discussion

3.1. Characterization of the adsorbent

Tilkitepe/Van basin has claystone formations which contain clay minerals and non-clay minerals such as smectite (montmorillonite), illite, quartz, calcite, feldspar, amorphous

material, mica (biotite), kaolin-serpentine group minerals, mixed layered clay mineral. The X-ray powder diffraction analyses of normal, glycolated and heat-treated raw clay samples are shown in Fig. 1.

The powder diffraction patterns indicate the predominance of quartz and calcite in the raw clayey material, with the most intense peaks, respectively, detected at 3.3619 and 3.0434 Å. A low quantity of feldspar is detected at 3.2063 Å. The positions of 001 reflection of the smectite and illite appear at 14.5868 and at 10.72 Å for the sample, respectively. The phases like kaolin-serpentine group minerals (reflection at 7.2695 Å), mixed layered clay mineral (reflection at 17.0623 Å) and mica (reflection at 10.1129 Å) are the minor phases.

The infrared spectra (Figs. 2(a) and (b)) are in the frequency range 4,000–400 cm^{-1}.

The distinct increase of infrared absorbency at 3,620–910 cm^{-1} confirms the dominant presence of dioctahedral smectite with [Al, Al–OH] stretching and bending bands [50]. The absorption bands at 3,200–3,800 cm^{-1} and at 1,600–1,700 cm^{-1} may be attributed to the OH frequencies for the water molecule adsorbed on the clay surface [51,52]. Fig. 2(a) shows the IR spectrum of the raw clayey material. The characteristic bands of the calcite mineral are 1,435.04, 871.82 and 713.66 cm^{-1}. The IR peaks at 1,797.66 and 2,515.18 cm^{-1} also indicate the presence of calcite and dolomite. The peak size at 1,435.04 cm^{-1} indicates that the sample has a high amount of calcite. The strong band at 1,018.41 cm^{-1} (depending on Si–O stretching) is the main characteristic band of quartz. And the other bands at 798.53 and 779.24 cm^{-1} also belong to quartz [53]. The band at 871.82 cm^{-1} attributed to Fe–Al–OH of montmorillonite [51,52]. The bands at 509.21 and 462.92 cm^{-1} are attributed to Si–O–Al and Si–O–Si bending vibrations, respectively [54]. The stretching vibration of the adsorbed water molecules is observed at 3,429.43 cm^{-1}. Another characteristic band for the bending vibrations of the adsorbed water appeared as a small band at 1,635.64 cm^{-1}. The stretching vibrations of the surface hydroxyl groups (Si–Si–OH or Al–Al–OH) are observed at 3,564.45 cm^{-1} [54]. The IR peaks belonging to the C–H stretching vibrations of the organic materials naturally found in the sample are observed at 2,985.81 and 2,873.94 cm^{-1} [55]. Fig. 2(b) shows the IR spectrum obtained after Cu(II) and Cd(II) adsorption. Some shifts in the wavelengths indicate that metals are bonded on the surface of the adsorbent. There are clear shifts in the wave numbers from 3,564.45 cm^{-1} (raw clayey material) to 3,576.02 cm^{-1} (metal loaded raw clayey material) and from 3,429.43 cm^{-1} (raw clayey material) to 3,441.01 cm^{-1} (metal loaded raw clayey material). This shows that –OH groups on the surface of the adsorbent are responsible for the adsorption of metal ions [56]. The vibration at 2,360 cm^{-1} is attributed to CO_2 [57] from the air during the pellet construction and is not taken into consideration.

The DTA peak temperatures are characteristic for each mineral and DTA curves are applicable for the identification and determination of many types of clay [58]. TG–DTA curves of the raw clay are given in Fig. 3 for the temperature range of 10°C–1,100°C.

Thermal methods enable to study the different steps of weight loss due to release of adsorbed water (dehydration reactions), OH (dehydroxylation reactions) and CO_2 (decarbonation reactions) [50]. In the DTA curves, at low temperature 118°C, an endothermic reaction occurs due to the removal of the physically bound water [59]. A small endothermic peak between 360°C and 480°C corresponds to the loss of interlayer water from the clay mineral structure. Clays can be described as polymineral formations. The effects of the components within the mixture may be in various situations. According to Yalçin [60], it is determined that the dehydration temperatures of clay samples are different which starts at 130°C in illite clay, at 220°C in montmorillonite clay and at 420°C in hydromica clay. As the temperature

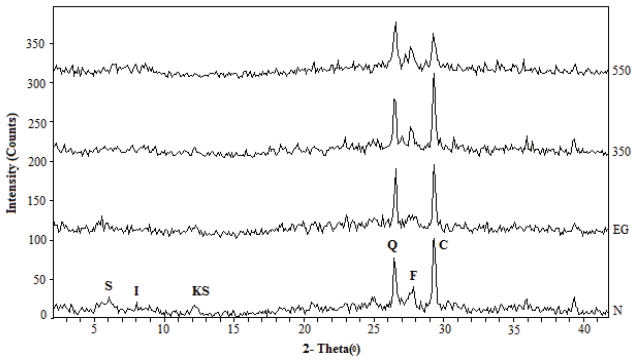

Fig. 1. X-ray patterns of the raw material sample. Normal (N), ethylene glycolated (EG) and heated at 350°C and 550°C (S: Smectite, I: Illite, K: Kaolinite, Q: Quartz, C: Calcite, F: Feldspar).

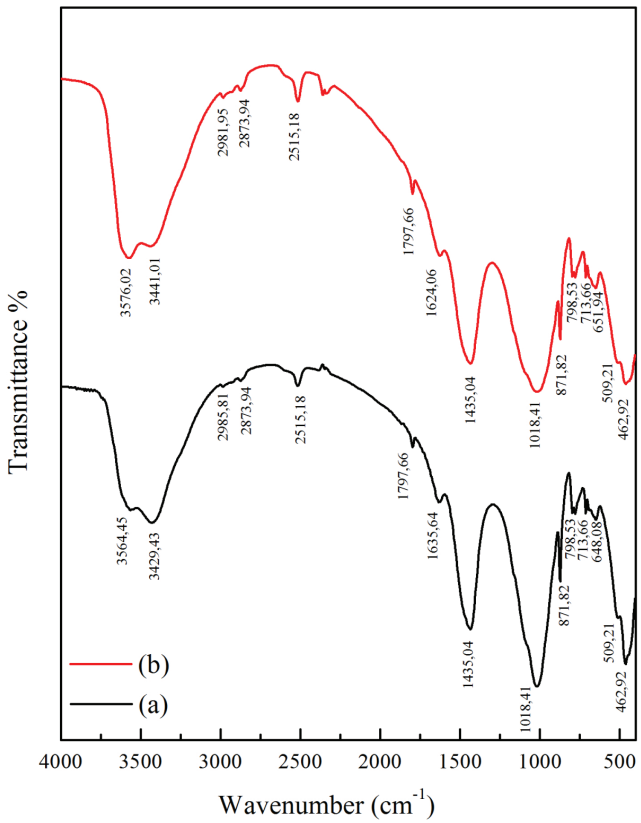

Fig. 2. FTIR spectrum of raw material (a) and metal loaded clayey material (b) from Tilkitepe.

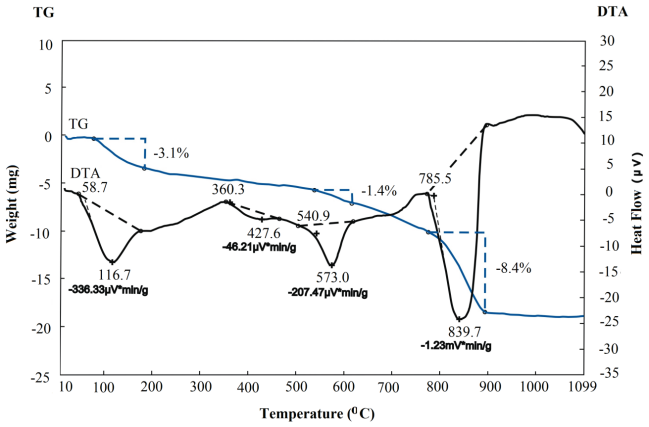

Fig. 3. TG–DTA curve of raw sample.

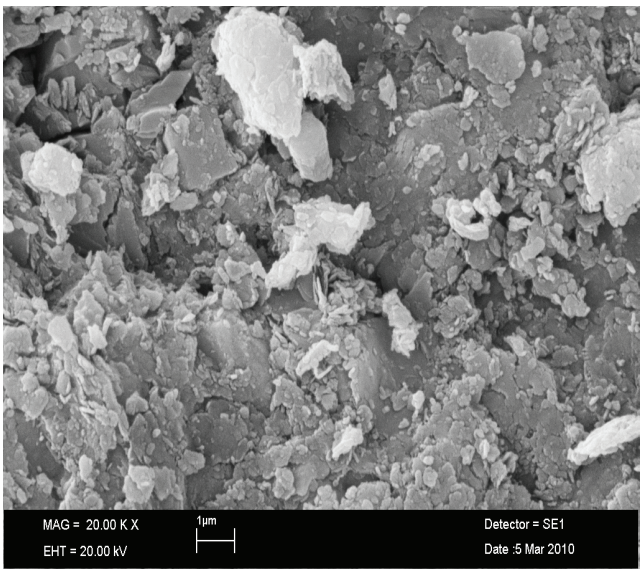

Fig. 4. Scanning electron microphotograph of the raw material.

increases, an endothermic band occurs at 573°C for sample was due to the dehydroxylation of the clay minerals and the $\alpha \rightarrow \beta$ quartz transformation [61,62] and other endothermic peak that appears at 839°C can be attributed to the carbonate decomposition [63]. After about 900°C appears weak various exothermic effects, belong to crystallization of high temperature phases [64].

The TG curve of the original sample shows three main steps of weight loss. The mass losses of 3.1%, 1.4% and 8.4% belongs to the dehydration, dehydroxylation and decarbonation reactions, respectively. The first loss of weight occurs between 38°C and 170°C. This transformation is due to the removal of adsorbed and interlayer water from the clay mineral. Then, the TG curve shows a slight gradual decline in the range of 170°C–540°C, which is attributed to the water loss of clay minerals. Finally, a third main loss occurs at temperatures in the range of 785°C–900°C related to the breakdown of carbonates with high CO_2 releasing as a component of the fluid phase [64].

The examination of microstructure by scanning electron microscope is presented in Fig. 4.

The raw clay consists mostly of spherical shaped and aggregate that contains varying sizes and amount of particles.

3.2. *Adsorption isotherms*

Adsorption isotherm provides valuable information such as equilibrium sorption capacity and certain constants whose values express the surface properties and affinity of the adsorbent [65].

The experimental data were applied on non-linear Langmuir, Freundlich, DKR, Temkin and Harkins–Jura adsorption models successively, using equations in Table 2. Figs. 5(a) and (b) illustrate the adsorption equilibrium isotherms used for the adsorption of Cu(II) and Cd(II) ions by using raw material in binary metal system.

It shows the relationship between the amount of metal ions adsorbed onto the adsorbent surface and the metal ion concentration in the aqueous phase at equilibrium [19]. The values of parameters and the correlation coefficients of non-linearized isotherm models are given in Tables 3(a) and (b) for Cu(II) and Cd(II) ions adsorption at different temperatures.

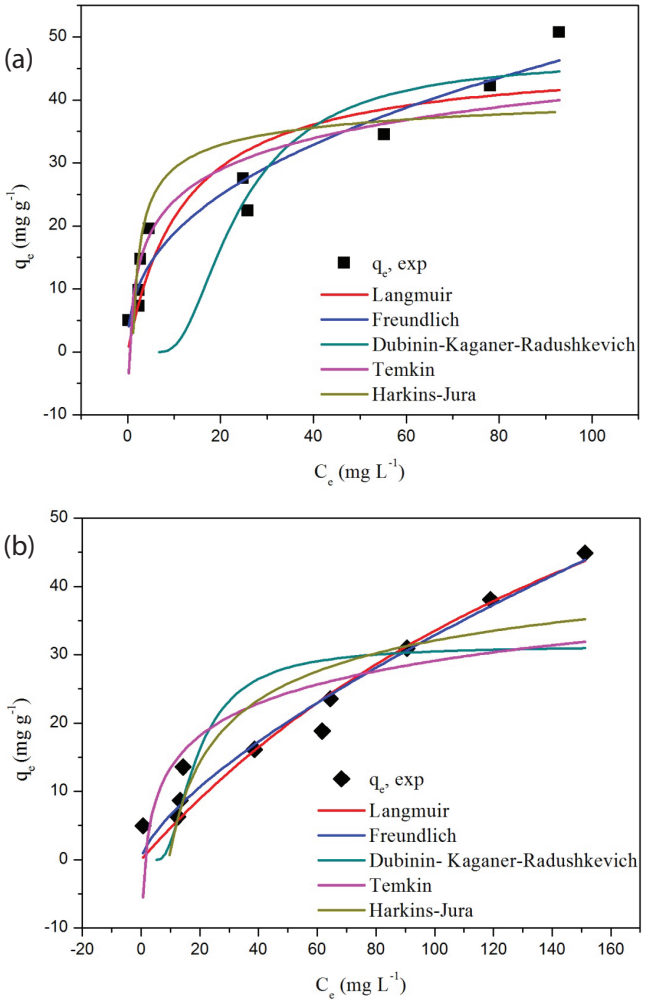

Fig. 5. The comparison of non-linear isotherm models with experimental data for the adsorption of (a) Cu(II) ions and (b) Cd(II) ions onto adsorbent at 298 K.

Table 3(a)
Isotherm parameters of Cu(II) adsorption onto raw material obtained by non-linear method

Isotherm/model		298 K		308 K		318 K	
		Value	SE	Value	SE	Value	SE
Langmuir	q_m (mg g^{-1})	46.9584	6.06056	61.4536	8.6085	29.8494	3.7702
	K_L	0.0828	0.03942	0.0115	0.0033	0.0246	0.0098
	R_L	0.1945	–	0.6335	–	0.4479	–
	R^2	0.8349	–	0.9513	–	0.7932	–
	χ^2	3.8029	–	1.3401	–	4.5147	–
Freundlich	K_F	7.4277	1.3884	2.2531	0.3368	3.0639	1.2024
	$1/n$	0.4034	0.2910	0.5740	0.0995	0.3943	0.5088
	R^2	0.9387	–	0.9839	–	0.7957	–
	χ^2	0.0991	–	0.0279	–	1.6318	–
Dubinin–Kaganer–Radushkevich	q_m (mg g^{-1})	46.8100	18.8683	20.4875	4.6954	24.3600	2.6320
	β	0.0463	0.1280	0.1540	1.3219	0.1252	0.0912
	E_{DKR} (kJ mol^{-1})	5.4347	–	1.6233	–	1.9968	–
	R^2	0.4710	–	0.8113	–	0.66545	–
	χ^2	12.434	–	1.0080	–	1.6726	–
Temkin	q_m (mg g^{-1})	0.2780	16.824	0.3439	6.7242	0.2587	8.8892
	b_T	9.5917	5.8355	8.4707	1.0186	10.014	1.0073
	A_T	2.8138	1.1079	0.2388	0.0572	0.2418	0.9345
	R^2	0.7941	–	0.9024	–	0.7872	–
	χ^2	4.8387	–	1.1706	–	1.9962	–
Harkins–Jura	A	111.10	4.182	440.46	1.490	336.04	0.0128
	B	6.8764	3.3451	3.4114	1.5748	2.0903	0.9828
	R^2	0.7933	–	0.7907	–	0.7846	–
	χ^2	0.4857	–	0.3587	–	0.1376	–

The Langmuir isotherm parameters presented in Tables 3(a) and (b) for binary adsorption system at 298 K give a low value of R^2 for both Cu(II) (0.8349) and Cd(II) (0.8919) indicates that the adsorption process exactly may not be explained this model. Maximum adsorption capacities and SEs are determined as q_m = 46.9584 (mg g^{-1}) and q_m = 81.6038 (mg g^{-1}), and SE = 6.06056 and SE = 3.5874, respectively, for Cu(II) and Cd(II) ions onto adsorbent in binary system. Also, χ^2 values are calculated as 3.8029 and 1.3800, respectively, for both adsorbates. The values of R_L for competitive adsorption of Cu(II)–Cd(II) on raw material surface are between 0 and 1, which indicates favorable adsorption of these ions on surface of Tilkitepe raw materials. The adsorption coefficients, K_L value that is related to the apparent energy of sorption for Cu(II) was greater than those of Cd(II) [25,66].

The Freundlich isotherm gives a better fit particularly for Cd(II) adsorption from solution (correlation coefficient, R^2 = 0.9538). For a good adsorbent, the value of $1/n$ expected to be in the range from 0.4 to 0.9. A smaller value of $1/n$ indicates better adsorption and formation of comparatively strong bond between the adsorbate and adsorbent. From the $1/n$ values (Tables 3(a) and (b)), it is observed that raw material adsorbs Cu(II) stronger than Cd(II) [67]. Also, Freundlich isotherm constants (K_F) 7.4277 and 1.3013, SEs 1.3884 and 0.4319, and χ^2 values 0.0991 and 0.0006 were determined, respectively, for competitive adsorption of Cu(II) and Cd(II) ions onto adsorbent. $1/n$ and χ^2 values are close to zero and also R^2 values being close to 1 show that adsorption of Cu(II) and Cd(II) ions on the Tilkitepe raw material can be better explained with Freundlich isotherm than Langmuir isotherm.

DKR adsorption isotherm is not good in the present study (R^2 = 0.4710 for Cu(II) adsorption and 0.5886 for Cd(II) adsorption onto adsorbent). Adsorption energy (E) values are lower than 8 kJ mol^{-1} indicates that the adsorption mechanism is a combination of electrostatic interaction and physical adsorption [68]. The values of the parameter E (Tables 3(a) and (b)) for Cu(II) are found to be more than that for Cd(II).

Table 3(b)
Isotherm parameters of Cd(II) adsorption onto raw material obtained by non-linear method

Isotherm/model		298 K		308 K		318 K	
		Value	SE	Value	SE	Value	SE
Langmuir	q_m (mg g^{-1})	81.6038	3.5874	108.161	4.0570	51.0712	5.4931
	K_L	0.0066	0.0044	0.0044	0.0024	0.0055	0.0011
	R_L	0.7507	–	0.8166	–	0.7815	–
	R^2	0.8919	–	0.9320	–	0.9735	–
	χ^2	1.3800	–	1.0132	–	0.0002	–
Freundlich	K_F	1.3013	0.4319	0.3094	0.1630	0.9750	0.2667
	$1/n$	0.7010	0.1489	0.9383	0.1249	0.6224	0.1375
	R^2	0.9538	–	0.9453	–	0.9579	–
	χ^2	0.0006	–	0.0072	–	0.0003	–
Dubinin–Kaganer–Radushkevich	q_m (mg g^{-1})	31.3367	5.4910	0.3914	0.0872	0.2750	0.0217
	β	0.2047	1.2736	0.5564	7.8745	0.1206	39.3652
	E_{DKR} (kJ mol^{-1})	1.2212	–	0.4493	–	2.0729	–
	R^2	0.5886	–	0.8067	–	0.9271	–
	χ^2	0.0029	–	0.0025	–	0.0005	–
Temkin	q_m (mg g^{-1})	0.2697	6.7812	0.3918	5.5140	0.0338	2.7321
	b_T	9.7780	1.6727	7.8563	1.6672	8.5587	1.7702
	AT	0.7166	0.6588	0.0803	0.0225	0.0726	0.0104
	R^2	0.5651	–	0.7810	–	0.9491	–
	χ^2	8.1065	–	3.6475	–	4.8530	–
Harkins–Jura	A	110.47	0.4161	167.35	0.7599	100.62	2.4387
	B	1.1755	0.6157	1.9660	1.2582	9.2183	3.1393
	R^2	0.7884	–	0.6975	–	0.8826	–
	χ^2	0.3554	–	1.3375	–	0.8958	–

The Temkin isotherm plots (Figs. 5(a) and (b)) and parameters (Tables 3(a) and (b)) show that the model cannot define sufficiently the adsorption isotherms of Cu(II) and Cd(II) ions onto raw material. The correlation coefficients are not good in the present study (R^2 = 0.7941 for Cu(II) ion and R^2 = 0.5651 for Cd(II) adsorption onto raw material). The low values (9.5917 for Cu(II) ions and 9.7780 for Cd(II) ions) of the Temkin constant b_T (J mol^{-1}) show a weak adsorbate–adsorbent interaction [35].

Harkins–Jura isotherm plots for the experimental data are given in Figs. 5(a) and (b) for Cu(II) and Cd(II) ion adsorption. The related non-linear parameters are listed in Tables 3(a) and (b). The χ^2 and SE values for this model are 0.4857 and 4.182 for Cu(II), 0.3554 and 0.4161 for Cd(II), respectively, which are higher than Freundlich isotherm models. The values of R^2, for Cu(II) (0.7933) and Cd(II) (0.7884) at 298 K show that the adsorption process not follows this model.

In binary adsorption process, metals are in competition for the same sorbent active sites. In this case, a greater affinity metals (strongly adsorbed species) can displace others with a lower affinity (weakly adsorbed species) [69]. The experimental results exhibited that higher adsorption of Cu(II) ions when compared with Cd(II) ions. This indicates that the affinity of the adsorbent for adsorption of the metal ions followed the order of Cu(II) >> Cd(II). This can be explained by ionic radius (0.73 Å Cu^{2+} < 0.95 Å Cd^{2+}), hydrated ionic radius (4.19 Å Cu^{2+} < 4.26 Å Cd^{2+}) and electronegativity (1.90 Cu^{2+} > 1.69 Cd^{2+}) of studied metal ions [19,70]. The adsorption capacity of this adsorbent in the binary system has been compared with some alternative adsorbents reported in the literature (Table 4).

3.3. The effect of pH on adsorption

The pH of the aqueous solution is a significant parameter affecting the adsorption of the metal at the adsorbent–solution interfaces [76]. Metal ions in aqueous solutions can be hydrated or can hydrolyze according to the reactions:

Table 4
Maximum adsorption capacity of various adsorbent samples for adsorption of Cu(II) and Cd(II) ions reported in the literature

Adsorbent	Cu(II) (q_m)	Cd(II) (q_m)	Adsorption system	Reference
Bentonite	–	0.692 (meq g^{-1})	Cd(II)–Ni(II)	[71]
Vermiculite	0.513 (meq g^{-1})	–	Pb(II)–Cu(II)	[71]
Activated carbon	4.77 (mg g^{-1})	–	Cu + Cd	[72]
Kaolin	4.36 (mg g^{-1})	–	Cu + Cd	[72]
Bentonite	7.56 (mg g^{-1})	5.80 (mg g^{-1})	Cu + Cd	[72]
Diatomite	4.27 (mg g^{-1})	–	Cu + Cd	[72]
Compost	8.90 (mg g^{-1})	5.36 (mg g^{-1})	Cu + Cd	[72]
Anaerobic sludge	–	8.94 (mg g^{-1})	Cu + Cd	[72]
Cellulose pulp waste	4.55 (mg g^{-1})	1.82 (mg g^{-1})	Cu + Cd	[72]
Natural clay RY	–	3.61 (mg g^{-1})	Pb(II)–Cd(II)	[73]
Natural clay RS	–	1.15 (mg g^{-1})	Pb(II)–Cd(II)	[73]
Natural clay RY	11.14 (mg g^{-1})		Pb(II)–Cu(II)	[73]
Natural clay RS	8.62 (mg g^{-1})		Pb(II)–Cu(II)	[73]
Nanoparticle agglomerates of titanium(IV) oxide (NHTO)	44.81 (mg g^{-1}) (T = 30°C)	55.62 (mg g^{-1}) (T = 30°C)	Cd(II)–Cu(II)	[74]
Tea-industry waste	6.65 ± 0.31 (mg g^{-1})	2.59 ± 0.26 (mg g^{-1})	Cd(II)–Cu(II)	[75]
Surface-modified nanoscale carbon black	341 ± 30.7 (mmol kg^{-1}) 1.0 mM Cd(II)	278 ± 15.0 (mmol kg^{-1}) 1.0 mM Cu(II)	Cd(II)–Cu(II)	[76]
Local raw clayey material	52.631 (mg g^{-1})	44.843 (mg g^{-1})	Cd(II)–Cu(II)	This study

$M^{2+} + nH_2O \leftrightarrow M(H_2O)\ n^{2+}$ or $M_{aq}^{2+} + nH_2O \leftrightarrow M(OH)^{2-n} + nH^+$

Hydroxometal complexes are known to adsorb with a higher affinity than the fully hydrated metals [77]. According to Srivastava et al. [2], each type of cadmium and copper metal in solution is almost identical in single and multielement system. Cd^{2+} species up to a pH 8.5 and Cu^{2+} species up to pH 6.0 are the dominant in the solution, after which its concentration decreases. Concentration of the various Cu hydroxyl species improves above pH 6.0 in both the systems [2]. In this study, the pH value of aqueous suspension of the raw clay sample was measured as 8.1. This value of pH is not suitable for adsorption of Cd^{2+} and Cu^{2+} ions onto clay.

The adsorption properties of clay minerals or mineral mixtures are related to the net negative charge of the mineral structure [78]. A pH value exists at which the sum of negative charges equals the sum of positive charges and the net charge of the surface is zero (pzc). The point of zero charge (pH_{pzc}) is an important adsorbent parameter that aids in understanding the adsorption of charged species and the influence of pH on the adsorption process. Generally, the adsorption of charged species onto charged surfaces can be expected to be strongly influenced by electrostatic attraction or repulsion forces [78]. Three main mechanisms are separated for the interaction of metals with the surface of raw clay particles: (1) Coulomb interactions occur between metal ions (hydrated cations, hydroxo and other complexes) with the charged surface. The metal is completely dissociated and retained in the surface diffuse layer by electrostatic attraction forces, but retains mobility and ability to move in the near-surface solution volume. (2) The formation of localized outer-sphere complexes of hydrated metal ions with surface functional groups. Metals bound to the surface by the first two ways belong to non-specifically sorbed (exchangeable) cations, which can be displaced by other cations. (3) The specific sorption of metals with the formation of strong covalent bonds with the functional groups of organic and inorganic components of raw clay material (inner-sphere complexes). Metal cations occur in the dense part of the double electric layer. Such adsorption can occur even on a likely charged surface, in spite of the generated Coulomb repulsion [79].

The pH_{pzc} value of the raw clay determined by potentiometric titrations as ~3.00. When the solution pH was above the pH_{pzc}, the adsorbent surface had a negative charge, while at low pH (pH_{pzc}) it has a positive charge. The pH_{pzc} was recognized as the pH where 0.1 M HNO_3 titration curves of different raw clay masses (0.15, 0.20 and 0.45 g suspended in 0.03 M KNO_3 at pH 12.0) converged with that of the reactive bare solution [68]. As a result of all assessments, optimum pH value was selected as 5.5 in this study. Thus, the adsorbent surface may also be negatively charged, providing adsorption sites for Cu(II) and Cd(II) ions. Srivastava et al. [2] suggest that transition metals adsorb at permanent- and variable-charge sites. The variable-charge sites can undergo both protonation and deprotonation reactions. Adsorption at permanent-charge sites predominated up to pH 5.5 and 7.0 for Cu and Cd, respectively, in the multielement systems [2,80]. Permanent negatively charged sites on raw clay surfaces take place from isomorphous substitution, despite these sites are usually much less abundant than variable-charge sites at the edges. These permanent charges are neutralized by the adsorption of cations from the background electrolyte to form outer-sphere complexes [81]:

$$M^{2+} + 2X^-. . . .Na^+ = X_2M + 2Na^+$$

where M^{2+} represents the metal cation, X^- is a permanent negatively charged site and X_2M is an outer-sphere complex in the model of Srivastava et al. [2].

3.4. Adsorption kinetics

Solid–liquid adsorption process involves solute transfer, which is generally explained by either external mass transfer (boundary layer diffusion) or intraparticle diffusion or both. By the kinetic models, it is possible to determine the steps that control the adsorption process. Five different kinetic models which is detailed in section 2.5, including linearized pseudo-first-order, pseudo-second-order, intraparticle diffusion, Avrami and mass transfer kinetic models were applied to fit the experimental data obtained from the binary adsorption system (Figs. 6(a)–(e)) and the kinetic parameters were listed in Table 5 [4].

The calculations have been done for 50, 75, 100, 150, 200, 250, 300, 400, 500 and 600 mg L^{-1} initial concentration in binary system at 298 K. Values of adsorption kinetic parameters are calculated from the corresponding slopes and intercepts of the a straight-line graph. The linearity of the pseudo-first-order plots was not very high (Table 5). Therefore, pseudo-first-order plots not presented [37] in this study.

Straight lines are provided from the graph of t/q_t vs. t by using pseudo-second-order model (Fig. 6(a) for Cu(II) and Fig. 6(b) for Cd(II) ions). In the kinetic evaluation study for both ions adsorption, Cd (II) and Cu (II), the linear regression correlations (R^2) from pseudo-second-order model were

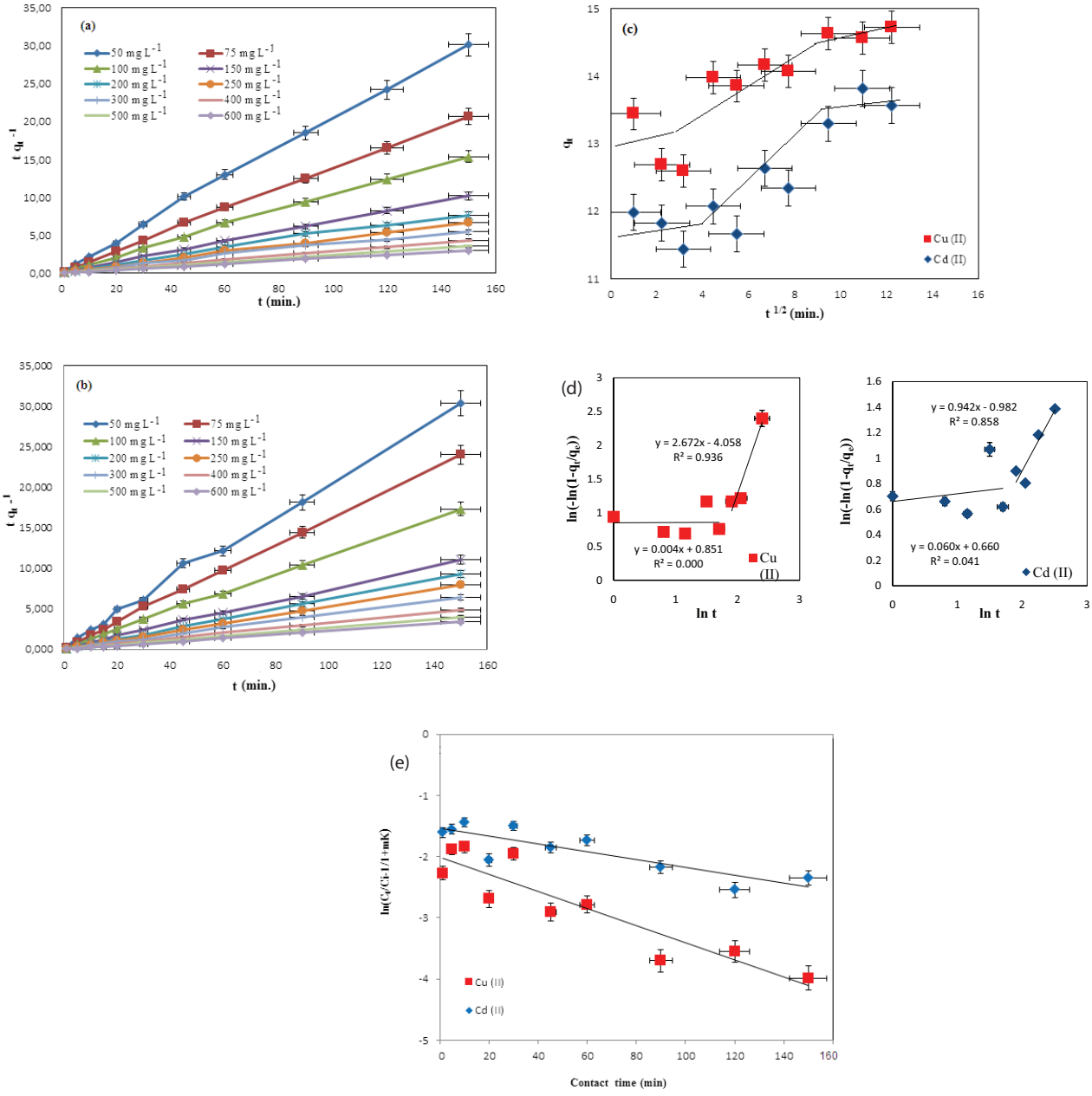

Fig. 6. Pseudo-second-order adsorption kinetics of (a) Cu(II) and (b) Cd(II) (T = 298 K), and (c) intraparticle diffusion plots, (d) Avrami and (e) mass transfer kinetic model for adsorption of Cu(II) and Cd(II) ions onto raw material in binary system (C_i = 150 mg L^{-1}, T = 298 K).

Table 5
Intraparticle diffusion, mass transfer, pseudo-first-order and pseudo-second-order kinetic parameters of Cu(II) and Cd(II) adsorption onto raw material at various initial metal ions concentrations in binary system (T = 298 K)

Metal ions	Initial metal concentration (mg L^{-1})	q_e experimental (mg g^{-1})	Pseudo-first-order model			Pseudo-second-order model			Intraparticle diffusion model		Mass transfer model	
			q_e calculated (mg g^{-1})	k_1 (min^{-1})	R^2	q_e calculated (mg g^{-1})	k_2 (g mg^{-1} min^{-1})	R^2	k_i (mg g^{-1} $min^{-0.5}$)	R^2	β (m s^{-1})	R^2
Cu(II)	50	4.977	0.655	0.086	0.8754	5.000	0.014	0.9992	0.184	0.9700	2.5999E–05	0.3050
	75	7.259	0.561	0.100	0.9140	7.288	0.149	0.9997	0.200	0.9410	1.3424E–05	0.7373
	100	9.756	1.710	0.081	0.8785	9.775	0.090	0.9993	0.150	0.9710	1.8692E–05	0.6299
	150	14.719	3.750	0.061	0.8671	14.814	0.048	0.9997	0.542	0.9600	2.3790E–05	0.8416
	200	19.540	17.049	0.040	0.7693	19.455	0.021	0.9968	0.422	0.8850	1.8352E–05	0.6421
	250	22.412	3.529	0.416	0.0939	22.522	0.046	0.9989	0.965	0.9960	5.9475E–05	0.3983
	300	27.511	13.231	0.058	0.2477	27.548	0.014	0.9953	1.623	0.9270	7.4769E–06	0.3072
	400	34.474	2.377	0.018	0.0443	34.722	0.029	0.9995	0.748	0.9690	4.2482E–06	0.5454
	500	42.193	22.855	0.024	0.3565	42.194	0.072	0.9999	0.177	0.9980	2.0391E–06	0.4438
	600	59.070	22.044	0.024	0.2844	52.631	0.017	0.9987	0.854	0.9390	1.5293E–06	0.1016
Cd(II)	50	4.938	0.146	0.055	0.3565	5.001	0.099	0.9972	0.739	0.9370	2.9723E–06	0.4537
	75	6.251	0.218	0.003	0.1145	6.269	0.206	0.9996	0.092	0.9820	2.3312E–07	0.0945
	100	8.667	2.303	0.006	0.5650	8.726	0.097	0.9999	0.300	0.9780	5.828E–07	0.6736
	150	13.568	10.602	0.016	0.7554	13.755	0.039	0.9987	0.467	0.9120	9.3251E–07	0.7354
	200	16.144	0.515	0.002	0.0612	16.155	1.596	0.9997	0.233	0.9550	1.8941E–07	0.1354
	250	18.832	2.615	0.239	0.2297	18.832	0.148	0.9997	1.315	0.9820	2.9141E–08	0.0151
	300	23.557	3.630	0.011	0.0128	23.364	0.084	0.9984	0.299	0.8260	7.2852E–08	0.0179
	400	30.954	1.541	0.013	0.1841	30.959	0.057	0.9998	0.568	0.7180	8.7423E–08	0.0344
	500	38.097	2.682	0.115	0.4139	38.167	0.361	1.000	1.030	0.8390	4.3711E–08	0.0490
	600	44.880	3.890	0.046	0.1076	44.843	0.037	0.9899	0.552	0.8080	7.1395E–08	0.0575

Table 6
Thermodynamic parameters for the adsorption of Cu(II) and Cd(II) onto raw clayey material

	C_i (mg L^{-1})	$\Delta H°$ (kJ mol^{-1})	$\Delta S°$ (kJ mol^{-1} K^{-1})	$\Delta G°$ (kJ mol^{-1})		
				298 K	308 K	318 K
Cu(II)	50	–145.3453	–447.2350	–12.0693	–7.5970	–3.1257
	75	–61.6259	–150.1145	–16.8918	–15.3906	–13.8895
	100	–94.5136	–286.6589	–9.0894	–6.2227	–3.3561
	150	–91.8863	–277.7458	–9.1181	–6.3406	–3.5631
	200	–82.1573	–247.5909	–8.3752	–5.8993	–3.4234
	250	–27.5950	–75.5194	–5.0902	–4.3550	–3.5798
	300	–91.0549	–286.0182	–5.8215	–2.9613	–0.1011
	400	–58.1864	–179.9981	–4.5470	–2.7470	–0.9470
	500	–57.1321	–177.6868	–4.1814	–2.0885	–0.6277
	600	–62.6418	–196.0691	–4.2132	–2.2525	–0.2918
Cd(II)	50	–133.4148	–415.9411	–9.4644	–5.3049	–1.1455
	75	–37.9908	–113.6940	–4.1100	–2.9730	–1.8361
	100	–32.7272	–95.3865	–4.3020	–3.3487	–2.3943
	150	–56.0098	–170.8860	–5.0858	–3.3769	–1.6681
	200	–29.1780	–86.8148	–3.3072	–2.4390	–1.5709
	250	–6.6852	–13.2409	–2.7394	–2.6070	–2.4746
	300	–31.2723	96.9994	–2.3665	–1.3965	–0.4273
	400	–30.3087	–91.6452	–2.9984	–2.0820	–0.2110
	500	–35.1075	–107.9739	–2.9313	–1.8515	–0.7718
	600	–37.1295	–114.8745	–2.8969	–1.7482	–0.5994

higher than those from pseudo-first-order model. Moreover, the calculated q_e values ($q_{e,cal}$) from the pseudo-second-order model were much closer to the experimental ones ($q_{e,exp}$). Hence, the pseudo-second-order model was more accurate to describe the competitive adsorption behavior of Cd^{2+} and Cu^{2+} [4]. The intraparticle diffusion plot is the plot of amount adsorbed per unit weight of sorbent, q_t (mg g^{-1}) vs. square root of time, $t^{1/2}$ is presented in Fig. 6(c). It is seen that the adsorption plots are not linear over the whole time range and can be divided into three linear stages which verify the multisteps of adsorption. The first linear region is attributed to physical adsorption (i.e., ion exchange) at the surface of the raw material, the second stage defines the gradual adsorption step, where intraparticle diffusion is rate limiting [67,68] and the third linear region indicated adsorption/desorption equilibrium. The rate constants, k_i (Table 5), have suggested that a large number of Cu(II) and Cd(II) ions may have diffused into the pores before being adsorbed [82]. Because the plots did not pass through the origin, proposing that intraparticle diffusion was not the merely rate-controlling step and the external mass transfer also provide an important contribution to the rate-controlling step owing to the big intercepts of the second linear region of the plots [4].

Avrami kinetic equation was also used to explain the mechanism of the adsorption process. Although the linearity of the plot (the linear coefficient values, R^2 not presented by the authors in the table) was insufficient, the authors determined the trend to a two-step adsorption process (Fig. 6(d)) [44]. The relatively first region of sorption can be ascribed to the mass transfer of Cu(II) and Cd(II) ions from the aqueous solution to the adsorbent surface. The regression values (0.0002 for Cu(II) and 0.0411 for Cd(II)) obtained is extremely low. The second part appears to be associated with the movement of metal ions or diffusion inside the pores of adsorbent and the interaction of the ions with the existing adsorption sites on the inner clay, binding the pore and capillary gaps [65]. The rate control mechanism of the adsorption process is not explained by using Avrami model in this study. The plot for the mass transfer model, $\ln[(C_t/C_i) - 1/(1 + mK)]$ vs. t is presented in Fig. 6(e).

The values of regression coefficient (R^2) and the mass transfer adsorption coefficient (β) are given in Table 5. This result indicates that this model for the adsorption system is not validity. When an evaluation is made among these models according to their R^2 values, pseudo-second-order kinetic model shows a better fit [83].

3.5. Adsorption thermodynamic

The thermodynamic data were calculated by using Eqs. (11)–(13) and listed in Table 6.

The Gibbs free energy change values $\Delta G°_{ads}$ are in the range of –12.0693 to –4.2132 kJ mol^{-1} and –9.4644 to –2.8969 kJ mol^{-1} for Cu(II) and Cd(II) at 298 K, respectively. These values show

that the adsorption process is spontaneous and regarded as a physical interaction. In addition, based on the decrease in negative $\Delta G°_{ads}$ values with increase in temperature, it can be resulted that the interaction between the Cu(II) and Cd(II) ions and adsorbent at higher temperatures is weaker and thus the adsorption is less favorable. The negative value of $\Delta H°_{ads}$ further approves the exothermic nature of the adsorption process of metal ions onto adsorbent. The negative value of $\Delta S°_{ads}$ shows the reduced randomness at the solid–solution interface during the adsorption process [43,84].

4. Conclusion

This study shows that Tilkitepe/Van raw clayey material can be used as an effective low cost adsorbent for heavy metal removal. The equilibrium adsorption data for Cu(II) and Cd(II) in binary solutions showed higher maximum adsorption capacity for Cu(II) when compared with Cd(II). The best models describing the kinetics and isotherms of binary adsorption are the pseudo-second-order kinetic and Freundlich model, respectively, which show the multilayer adsorption and clarifies the presence of heterogeneous pore distribution. The negative value of enthalpy change ($\Delta H°$) for both ions removal showed that the adsorption process is exothermic. Ion exchange is likely one of the main sorption mechanisms for binding divalent metal ions to the raw material.

References

[1] M.L. Sanchez, Causes and Effects of Heavy Metal Pollution, Nova Science Publishers, New York, USA, 2008, pp. 265–286.

[2] P. Srivastava, B. Singh, M. Angove, Competitive adsorption behavior of heavy metals on kaolinite, J. Colloid Interface Sci., 290 (2005) 28–38.

[3] A. Bourliva, K. Michailidis, C. Sikalidis, A. Filippidis, M. Betsiou, Adsorption of Cd(II), Cu(II), Ni(II) and Pb(II) onto natural bentonite: study in mono- and multi-metal systems, Environ. Earth Sci., 73 (2015) 5435–5444.

[4] C. Xiong, W. Wang, F. Tan, F. Luo, J. Chen, X. Qiao, Investigation on the efficiency and mechanism of Cd(II) and Pb(II) removal from aqueous solutions using MgO nanoparticles, J. Hazard. Mater., 299 (2015) 664–674.

[5] S. Sen Gupta, K.G. Bhattacharyya, Kinetics of adsorption of metal ions on inorganic materials: a review, Adv. Colloid Interface Sci., 162 (2011) 39–58.

[6] S. Yusan, C. Gok, S. Erenturk, S. Aytas, Adsorptive removal of thorium (IV) using calcined and flux calcined diatomite from Turkey: evaluation of equilibrium, kinetic and thermodynamic data, Appl. Clay Sci., 67–68 (2012) 106–116.

[7] M. Aivalioti, I. Vamvasakis, E. Gidarakos, BTEX and MTBE adsorption onto raw and thermally modified diatomite, J. Hazard. Mater., 178 (2010) 136–143.

[8] M. Rafatullah, O. Sulaiman, R. Hashim, A. Ahmad, Adsorption of methylene blue on low-cost adsorbents: a review, J. Hazard. Mater., 177 (2010) 70–80.

[9] K.R. Kumrić, A.B. Đukić, T.M. Trtić-Petrović, N.S. Vukelić, Z. Stojanović, J.D. Grbović Novaković, L.L. Matović, Simultaneous removal of divalent heavy metals from aqueous solutions using raw and mechanochemically treated interstratified montmorillonite/kaolinite clay, Ind. Eng. Chem. Res., 52 (2013) 7930–7939.

[10] L. Tran, P. Wu, Y. Zhu, L. Yang, N. Zhu, Highly enhanced adsorption for the removal of Hg(II) from aqueous solution by Mercaptoethylamine/Mercaptopropyltrimethoxysilane functionalized vermiculites, J. Colloid Interface Sci., 445 (2015) 348–356.

[11] S.M.I. Sajidu, I. Persson, W.R.L. Masamba, E.M.T. Henry, D. Kayambazinthu, Removal of Cd^{2+}, Cr^{3+}, Cu^{2+}, Hg^{2+}, Pb^{2+} and Zn^{2+} cations and AsO_4^{3-} anions from aqueous solutions by mixed clay from Tundulu in Malawi and characterisation of the clay, Water SA, 32 (2006) 519–526.

[12] Y. Ateş, T. Yakupoğlu, Assessment of lacustrine/fluvial clays as liners for waste disposal (Lake Van Basin, Turkey), Environ. Earth Sci., 67 (2012) 653–663.

[13] I. Ghorbel-Abid, M. Trabelsi-Ayadi, Competitive adsorption of heavy metals on local landfill clay, Arabian J. Chem., 8 (2015) 25–31.

[14] T.B. Musso, M.E. Parolo, G. Pettinari, F.M. Francisca, Copper and zinc adsorption capacity of three different clay liner materials from Argentina, J. Environ. Manage., 146 (2014) 50–58.

[15] V.K. Gupta, P.J.M. Carrott, M.M.L. Ribeiro Carrott, Suhas, Low-cost adsorbents: growing approach to wastewater treatment—a review, Crit. Rev. Environ. Sci. Technol., 39 (2009) 783–842.

[16] L. Järup, Hazards of heavy metal contamination, Br. Med. Bull., 68 (2003) 167–182.

[17] S. Çay, A. Uyanık, A. Özaşık, Single and binary component adsorption of copper(II) and cadmium(II) from aqueous solutions using tea-industry waste, Sep. Purif. Technol., 38 (2004) 273–280.

[18] Y. Yi, Z. Yang, S. Zhang, Ecological risk assessment of heavy metals in sediment and human health risk assessment of heavy metals in fishes in the middle and lower reaches of the Yangtze River basin, Environ. Pollut., 159 (2011) 2575–2585.

[19] R. Laus, V. Tadeu de Fávere, Competitive adsorption of Cu(II) and Cd(II) ions by chitosan crosslinked with epichlorohydrin–triphosphate, Bioresour. Technol., 102 (2011) 8769–8776.

[20] E. Konyar, P.A. Silva, Excavations at the Mound of Van Fortress/Tuspa, J. Acad. Marketing Mysticism Online, 3 (2011) 176–191.

[21] J. Wase, C. Forster, Biosorbents for Metal Ions, Taylor & Francis Ltd., e-Library, London, 2003, pp. 1–9.

[22] O. Amrhar, H. Nassalı, M.S. Elyoubi, Application of nonlinear regression analysis to select the optimum absorption isotherm for Methylene Blue adsorption onto Natural Illitic Clay, Bull. Soc. R. Sci. Liège, 84 (2015) 116–130.

[23] L.D. Gelb, K.E. Gubbins, Characterization of Porous Glasses by Adsorption: Models, Simulations and Data Inversion, F. Meunier, Ed., Fundamentals of Adsorption, 6th ed., Elsevier Paris, France, 1998, pp. 551–556.

[24] R. Varadarajan, G. Venkatesan, G. Swaminathan, Removal of copper using clay admixed with quarry fines as landfill liners, Pol. J. Environ. Stud., 25 (2016) 377–384.

[25] H.M. Baker, A study of the binding strength and thermodynamic aspects of cadmium and lead ions with natural silicate minerals in aqueous solutions, Desalination, 242 (2009) 115–127.

[26] I. Langmuir, The adsorption of gases on plane surfaces of glass, mica and platinum, J. Am. Chem. Soc., 40 (1918) 1361–1403.

[27] H.M.F. Freundlich, Over the adsorption in solution, Z. Phys. Chem., 57 (1906) 385–470.

[28] M.M. Dubinin, The potential theory of adsorption of gases and vapors for adsorbents with energetically nonuniform surfaces, Chem. Rev., 60 (1960) 235–241.

[29] O. Hamdaouia, E. Naffrechoux, Modeling of adsorption isotherms of phenol and chlorophenols onto granular activated carbon. Part I. Two-parameter models and equations allowing determination of thermodynamic parameters, J. Hazard. Mater., 147 (2007) 381–394.

[30] M. Hadi, M.R. Samarghandi, G. McKay, Equilibrium two-parameter isotherms of acid dyes sorption by activated carbons: study of residual errors, Chem. Eng. J., 160 (2010) 408–416.

[31] X. Chen, Modeling of experimental adsorption isotherm data, Information, 6 (2015) 14–22. doi:10.3390/info6010014.

[32] M. Brdar, M. Šćiban, A. Takaci, T. Dosenovic, Comparison of two and three parameters adsorption isotherm for Cr(VI) onto Kraft lignin, Chem. Eng. J., 183 (2012) 108–111.

[33] B. Subramanyam, A. Das, Linearised and non-linearised isotherm models optimization analysis by error functions and statistical means, J. Environ. Health Sci. Eng., 12 (2014) 92–97.

[34] K.Y. Foo, B.H. Hameed, Insights into the modeling of adsorption isotherm systems, Chem. Eng. J., 156 (2010) 2–10.
[35] M.S. Rahman, K.V. Sathasivam, Heavy metal adsorption onto *Kappaphycus* sp. from aqueous solutions: the use of error functions for validation of isotherm and kinetics models, Biomed. Res. Int., 2015 (2015) 1–13, doi: 10.1155/2015/126298.
[36] M.R. Samarghandi, M. Hadi, S. Moayedi, F.B. Askari, Two-parameter isotherms of methyl orange sorption by pinecone derived activated carbon, Iran. J. Environ. Health Sci. Eng., 6 (2010) 285–294.
[37] N.A. Oladoja, I.O. Asia, C.O. Aboluwoye, Y.B. Oladimeji, A.O. Ashogbon, Studies on the sorption of basic dye by rubber (*Hevea brasiliensis*) seed shell, Turk. J. Eng. Environ. Sci., 32 (2008) 143–152.
[38] A.O. Dada, A.P. Olalekan, A.M. Olatunya, O. Dada, Langmuir, Freundlich, Temkin and Dubinin–Radushkevich isotherms studies of equilibrium sorption of Zn^{2+} unto phosphoric acid modified rice husk, J. Appl. Chem., 3 (2012) 38–45.
[39] S. Tunali Akar, Y. Yetimoglu, T. Gedikbey, Removal of chromium (VI) ions from aqueous solutions by using Turkish montmorillonite clay: effect of activation and modification, Desalination, 244 (2009) 97–108.
[40] K.P.D. Iyer, A.S. Kunju, Extension of Harkins—Jura adsorption isotherm to solute adsorption, Colloids Surf., 63 (1992) 235–240.
[41] M.B. Ibrahim, S. Sani, Comparative isotherms studies on adsorptive removal of Congo Red from wastewater by watermelon rinds and neem-tree leaves, Open J. Phys. Chem., 4 (2014) 139–146.
[42] A.R. Cestari, E.F.S. Vieira, J.D.S. Matos, D.S.C. dos Anjos, Determination of kinetic parameters of Cu(II) interaction with chemically modified thin chitosan membranes, J. Colloid Interface Sci., 285 (2005) 288–295.
[43] A. Omri, A. Wali, M. Benzina, Adsorption of bentazon on activated carbon prepared from Lawsonia inermis wood: equilibrium, kinetic and thermodynamic studies, Arabian J. Chem., 9 (2016) S1729–S1739.
[44] N.A. Oladoja, A critical review of the applicability of Avrami fractional kinetic equation in adsorption-based water treatment studies, Desal. Wat. Treat., 57 (2016) 15813–15825.
[45] A. Gaid, F. Kaoua, N. Mederres, M. Khodjsa, Surface mass transfer processes using activated date pits as adsorbent, Water SA, 20 (1994) 273–278.
[46] M. Dogan, M. Alkan, A. Türkyilmaz, Y. Özdemir, Kinetics and mechanism of removal of methylene blue by adsorption onto perlite, J. Hazard. Mater., 109 (2004) 141–148.
[47] Z. Aksu, Determination of the equilibrium, kinetic and thermodynamic parameters of the batch biosorption of nickel(II) ions onto *Chlorella vulgaris*, Process Biochem., 38 (2002) 89–99.
[48] Y.S. Li, C.C. Liu, C.S. Chiou, Adsorption of Cr(III) from wastewater by wine processing waste sludge, J. Colloid Interface Sci., 273 (2004) 95–101.
[49] F. Mohellebi, F. Lakel, Adsorption of Zn^{2+} on Algerian untreated bentonite clay, Desal. Wat. Treat., 57 (2016) 6051–6062.
[50] F. Ayari, E. Srasra, M. Trabelsi-Ayadi, Characterization of bentonitic clays and their use as adsorbent, Desalination, 185 (2005) 391–397.
[51] J. Madejová, P. Komadel, Baseline studies of the Clay Minerals Society Source Clays: infrared methods, Clays Clay Miner., 49 (2001) 410–432.
[52] M. Felhi, A. Tlili, M.E. Gaied, M. Montacer, Mineralogical study of kaolinitic clays from Sidi El Bader in the far north of Tunisia, Appl. Clay Sci., 39 (2008) 208–217.
[53] J.A. Gadsden, Infrared Spectra of Minerals and Related Inorganic Compounds, The Butterworth Group, England, 1975.
[54] J. Madejova, FTIR techniques in clay minerals studies: a review, Vib. Spectrosc., 31 (2003) 1–10.
[55] Y.S. Al-Degs, M.I. El-Barghouthi, A.A. Issa, M.A. Khraisheh, G.M. Walker, Sorption of Zn(II), Pb(II), and Co(II) using natural sorbents: equilibrium and kinetic studies, Water Res., 40 (2006) 2645–2658.
[56] T.K. Naiya, B. Singha, S.K. Das, FTIR Study for the Cr(VI) Removal from Aqueous Solution Using Rice Waste, 2011 International Conference on Chemistry and Chemical Process, IPCBEE, Vol. 10, IACSIT Press, Singapore, 2011.
[57] M. Celebi, M. Yurderi, A. Bulut, M. Kaya, M. Zahmakiran, Palladium nanoparticles supported on amine-functionalized SiO_2 for the catalytic hexavalent chromium reduction, Appl. Catal., B, 180 (2016) 53–64.
[58] S. Yariv, The role of charcoal on DTA curves of organo-clay complexes: an overview, Appl. Clay Sci., 24 (2004) 225–236.
[59] A. Chakchouk, B. Samet, T. Mnif, Study on the potential use of Tunisian clays as pozzolanic material, Appl. Clay Sci., 33 (2006) 79–88.
[60] A. Yalçin, The effects of clay on landslides: a case study, Appl. Clay Sci., 38 (2007) 77–85.
[61] S. Mahmoudi, E. Srasra, F. Zargouni, The use of tunisian barremian clay in the traditional ceramic ındustry: optimization of ceramic properties, Appl. Clay Sci., 42 (2008) 125–129.
[62] H. Celik, Technological characterization and industrial application of two Turkish clays for the ceramic industry, Appl. Clay Sci., 50 (2010) 245–254.
[63] J.R. Odilon Kikouama, K.L. Konan, A. Katty, J.P. Bonnet, L. Baldé, N. Yagoubi, Physicochemical characterization of edible clays and release of trace elements, Appl. Clay Sci., 43 (2009) 135–141.
[64] M.J. Trindade, M.I. Dias, J. Coroado, F. Rocha, Mineralogical transformations of calcareous rich clays with firing: a comparative study between calcite and dolomite rich clays from Algarve, Portugal, Appl. Clay Sci., 42 (2009) 345–355.
[65] E.N. Lopes, F.S.C. dos Anjos, E.F.S. Vieira, A.R. Cestari, An alternative Avrami equation to evaluate kinetic parameters of the interaction of Hg(II) with thin chitosan membranes, J. Colloid Interface Sci., 263 (2003) 542–547.
[66] D.J.L. Guerra, I. Mello, L.R. Freitas, R. Resende, R.A.R. Silva, Equilibrium, thermodynamic, and kinetic of Cr(VI) adsorption using a modified and unmodified bentonite clay, Int. J. Min. Sci. Technol., 24 (2014) 525–535.
[67] J.U. Kennedy Oubagaranadin, N. Sathyamurthy, Z.V.P. Murthy, Evaluation of Fuller's earth for the adsorption of mercury from aqueous solutions: a comparative study with activated carbon, J. Hazard. Mater., 142 (2007) 165–174.
[68] N. Caliskan, A.R. Kul, S. Alkan, E. Gokirmak Sogut, I. Alacabey, Adsorption of zinc(II) on diatomite and manganese-oxide-modified diatomite: a kinetic and equilibrium study, J. Hazard. Mater., 193 (2011) 27–36.
[69] C.A. Christophi, L. Axe, Competition of Cd, Cu, and Pb adsorption on goethite, J. Environ. Eng., 126 (2000) 66–74.
[70] F. Qin, B. Wen, X.Q. Shan, Y.N. Xie, T. Liu, S.Z. Zhang, S.U. Khan, Mechanisms of competitive adsorption of Pb, Cu, and Cd on peat, Environ. Pollut., 144 (2006) 669–680.
[71] E. Padilla-Ortega, R. Leyva-Ramos, J.V. Flores-Cano, Binary adsorption of heavy metals from aqueous solution onto natural clays, Chem. Eng. J., 225 (2013) 535–546.
[72] M. Ulmanu, E. Maranon, Y. Fernandez, L. Castrillon, I. Anger, D. Dumitriu, Removal of copper and cadmium ions from diluted aqueous solutions by low cost and waste material adsorbents, Water Air Soil Pollut., 142 (2003) 357–373.
[73] A. Sdiri, T. Higashi, R. Chaabouni, F. Jamoussi, Competitive removal of heavy metals from aqueous solutions by montmorillonitic and calcareous clays, Water Air Soil Pollut., 223 (2012) 1191–1204.
[74] S. Debnath, U.C. Ghosh, Equilibrium modeling of single and binary adsorption of Cd(II) and Cu(II) onto agglomerated nano structured titanium(IV) oxide, Desalination, 273 (2011) 330–342.
[75] D.M. Zhou, Y.J. Wang, H.W. Wang, S.Q. Wang, J.M. Cheng, Surface-modified nanoscale carbon black used as sorbents for Cu(II) and Cd(II), J. Hazard. Mater., 174 (2010) 34–39.
[76] H.H. El-Maghrabi, S. Mikhail, Removal of heavy metals via adsorption using natural clay material, J. Environ. Earth Sci., 4 (2014) 38–46.
[77] A. Adamczuk, D. Kołodyńska, Equilibrium, thermodynamic and kinetic studies on removal of chromium, copper, zinc and arsenic from aqueous solutions onto fly ash coated by chitosan, Chem. Eng. J., 274 (2015) 200–212.
[78] E. Worch, Adsorption Technology in Water Treatment, Fundamentals, Processes and Modeling, Walter de Gruyter GmbH & Co. KG, Berlin, Boston, 2012.

[79] T.M. Minkina, G.V. Motusova, O.G. Nazarenko, S.S. Mandzhieva, Air, Water and Soil Pollution Science and Technology: Heavy Metal Compounds in Soil: Transformation upon Soil Pollution and Ecological Significance, Nova Science Publishers, Inc., Hauppauge, NY, 2010, pp. 125–147.
[80] J. Ikhsan, B.B. Johnson, J.D. Wells, A comparative study of the adsorption of transition metals on kaolinite, J. Colloid Interface Sci., 217 (1999) 403–410.
[81] A.R. Kul, N. Caliskan, Equilibrium and kinetic studies of the adsorption of Zn(II) ions onto natural and activated kaolinites, Adsorpt. Sci. Technol., 27 (2009) 85–105.
[82] K.G. Bhattacharyya, S. Sen Gupta, Removal of Cu(II) by natural and acid-activated clays: an insight of adsorption isotherm, kinetic and thermodynamics, Desalination, 272 (2011) 66–75.
[83] A. Dixit, P.K. Mishra, M.S. Alam, MATEC Web of Conferences 64 (2016) 01001.
[84] A. Demirbas, A. Sari, O. Isildak, Adsorption thermodynamics of stearic acid onto bentonite, J. Hazard. Mater., 135 (2006) 226–231.